LETTERS

Protection of telomeres through independent control of ATM and ATR by TRF2 and POT1

Eros Lazzerini Denchi[1] & Titia de Lange[1]

When telomeres are rendered dysfunctional through replicative attrition of the telomeric DNA or by inhibition of shelterin[1], cells show the hallmarks of ataxia telangiectasia mutated (ATM) kinase signalling[2–4]. In addition, dysfunctional telomeres might induce an ATM-independent pathway, such as ataxia telangiectasia and Rad3-related (ATR) kinase signalling, as indicated by the phosphorylation of the ATR target CHK1 in senescent cells[2,5] and the response of ATM-deficient cells to telomere dysfunction[6,7]. However, because telomere attrition is accompanied by secondary DNA damage, it has remained unclear whether there is an ATM-independent pathway for the detection of damaged telomeres. Here we show that damaged mammalian telomeres can activate both ATM and ATR and address the mechanism by which the shelterin complex represses these two important DNA damage signalling pathways. We analysed the telomere damage response on depletion of either or both of the shelterin proteins telomeric repeat binding factor 2 (TRF2) and protection of telomeres 1 (POT1) from cells lacking ATM and/or ATR kinase signalling. The data indicate that TRF2 and POT1 act independently to repress these two DNA damage response pathways. TRF2 represses ATM, whereas POT1 prevents activation of ATR. Unexpectedly, we found that either ATM or ATR signalling is required for efficient non-homologous end-joining of dysfunctional telomeres. The results reveal how mammalian telomeres use multiple mechanisms to avoid DNA damage surveillance and provide an explanation for the induction of replicative senescence and genome instability by shortened telomeres.

The shelterin complex can be compromised through inhibition of TRF2, which, together with TRF1, anchors this complex onto the double-stranded telomeric DNA[1]. Shelterin also contains POT1, a single-stranded DNA-binding protein that is tethered to TRF1 and TRF2 through the POT1 binding partner TPP1 (previously TINT1, PTOP, PIP1). When TRF2 is compromised, telomeres elicit a robust DNA damage signal, which can be detected by their decoration with DNA damage factors, forming 'telomere dysfunction-induced foci'[4] (TIFs). The ATM kinase is activated[3,4,8,] leading to cell cycle arrest mediated by the tumour protein p53 and the cyclin-dependent kinase inhibitor p21 (ref. 9). To determine whether TRF2 loss can induce a DNA damage response in the absence of ATM, we generated $Atm^{-/-}$ mouse embryonic fibroblasts (MEFs)[10] carrying the conditional allele of the gene for TRF2 ($Terf2^{F/-}$). Cells were immortalized with SV40 large T antigen to bypass the cell cycle arrest that normally occurs in response to telomere damage. As shown previously, deletion of TRF2 from $Atm^{+/+}$ cells leads to the induction of TIFs (Fig. 1a, b and Supplementary Fig. 1a) and phosphorylation of Chk2 (Fig. 1c). In contrast, in $Atm^{-/-}$ cells, the formation of TIFs (Fig. 1a, b and Supplementary Fig. 1a) and phosphorylation of Chk2 (Fig. 1c) in response to TRF2 deletion were largely abrogated. The deletion of TRF2 from $Atm^{-/-}$ cells was confirmed by PCR (Supplementary Fig. 1b), immunofluorescence (Supplementary Fig. 1c), disappearance of repressor activator protein 1 (Rap1; Fig. 1c), a TRF2-interacting protein whose stability depends on TRF2 (refs 8, 11), and telomeric chromatin immunoprecipitation (ChIP; Supplementary Fig. 2).

The inability of $Atm^{-/-}$ cells to respond to TRF2 deletion indicated that the ATR kinase is not involved in the detection of this type of telomere dysfunction. Consistent with the absence of an ATR response, TRF2 deletion did not induce phosphorylation of Chk1 (Fig. 1d). However, recent data have indicated that ATR activation at double-stranded DNA breaks (DSBs) induced by irradiation might depend on ATM[12], raising the possibility that the ATR response to dysfunctional telomeres might also require ATM. To test the role of ATR further, we used a short hairpin RNA (shRNA) that diminished ATR protein levels and compromised ATR signalling as deduced from the lack of ultraviolet-induced Chk1 phosphorylation (Supplementary Fig. 3). This level of ATR inhibition had no effect on TIF formation or the phosphorylation of Chk2 after TRF2 deletion from $Atm^{+/+}$ cells (Supplementary Fig. 3a, b). We therefore conclude that the telomere damage generated by TRF2 loss primarily activates ATM, not ATR.

Unexpectedly, $Atm^{-/-}$ cells showed a 15-fold reduction in the rate of telomere fusion in response to deletion of TRF2 (Fig. 1e and Supplementary Fig. 4a). The effect of ATM status on non-homologous end joining (NHEJ) of dysfunctional telomeres was also detectable in genomic blots (Supplementary Fig. 4b). Whereas $Terf2^{-/-}Atm^{+/+}$ cells showed the expected appearance of large-molecular-weight fragments that are typical of fused telomeres, $Terf2^{-/-}Atm^{-/-}$ cells revealed a largely unchanged telomeric restriction fragment pattern. Furthermore, the 3′ telomeric overhang signal was unaffected by deletion of TRF2 from $Atm^{-/-}$ cells (Supplementary Fig. 4b). In contrast, $Terf2^{-/-}Atm^{+/+}$ cells showed a significant reduction in 3′ overhang signals, as expected from the tight link between 3′ overhang processing and NHEJ[8,13]. The role of ATM in the NHEJ of dysfunctional telomeres was verified by *in vivo* deletion of TRF2 from quiescent mouse hepatocytes using an *Mx*–Cre system[11]. In this setting, ATM deficiency also diminished the occurrence of the telomere fusions (Supplementary Fig. 5). We conclude that, in primary cells as well as in immortalized cells, ATM is required for the recognition and processing of dysfunctional telomeres generated by loss of TRF2.

These results raised the possibility that the ATR kinase is repressed by another component of shelterin. Because the activation of the ATR kinase involves the binding of the replication protein RPA to single-stranded DNA[14], we considered the possibility that POT1 could be this factor. In this regard, *Saccharomyces cerevisiae* cell division cycle-13 (Cdc13), a protein with similarities to POT1, represses signalling by mitosis entry checkpoint-1 (Mec1)[15–17]. To test the role of POT1 in repression of the ATR kinase, we used POT1-null MEFs. Rodents have two POT1 genes, *Pot1a* and *Pot1b*, both of which are required for telomere function[18]. Deletion of *Pot1a*, alone or with *Pot1b*,

[1]Laboratory for Cell Biology and Genetics, The Rockefeller University, 1230 York Avenue, New York, New York 10021, USA.

induces TIFs[18,19]. In contrast to the results with TRF2, the TIF response in *Pot1a/b* double knockout cells was significantly reduced when we inhibited ATR with shRNA (Fig. 2a, b). Furthermore, unlike TRF2-null cells, *Pot1a/b* double knockout cells showed phosphorylation of Chk1 as well as Chk2, consistent with ATR signalling, and the phosphorylation of these downstream kinases depended on ATR (Fig. 2c). The role of ATR in the DNA damage response elicited by loss of POT1a was corroborated by conditional deletion of ATR from MEFs[20] (Fig. 2d). Efficient ATR deletion was confirmed on the basis of diminished induction of Chk1 phosphorylation by ultraviolet irradiation (Fig. 2e). We used two approaches to remove POT1a from the telomeres of these cells: an shRNA that was previously shown to affect POT1a specifically[18,] and an shRNA that effectively knocks down TPP1 as monitored by ChIP[21]. Both approaches resulted in the formation of TIFs and, in both cases, Cre-mediated deletion of ATR significantly suppressed the telomere damage response (Fig. 2d). In contrast, the status of ATM expression in the cells did not affect the response to the type of telomere damage induced by POT1a or TPP1 knockdown (Supplementary Fig. 6a–c). To test whether POT1 represses ATR signalling at telomeres of human cells, we used a colon carcinoma cell line (HCT116) with a conditional *ATR* allele[22]. The cells were infected with a *POT1* shRNA that has been shown to elicit a telomere damage response[23].

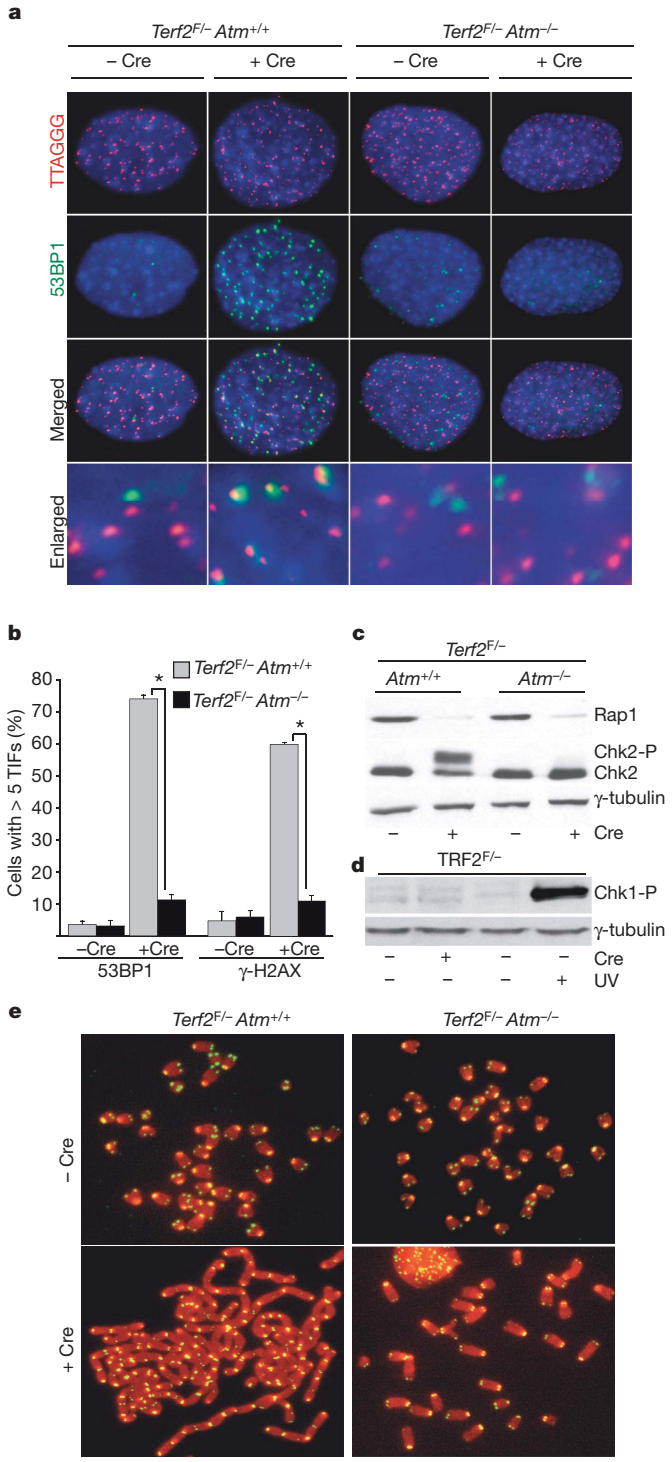

Figure 1 | TRF2 deletion activates ATM, not ATR. **a**, 53BP1-positive TIFs in MEFs of the indicated genotypes (DNA stained with DAPI (blue)). **b**, Quantification of 53BP1- and γH2AX-positive TIFs (mean and s.d. of triplicate experiments; $n \geq 150$; asterisk, $P < 0.001$ calculated using a two-tailed Student's *t*-test). **c**, **d**, Immunoblots showing Rap1 and Chk2 (**c**), and Chk1 phosphorylation induced by ultraviolet irradiation (25 J m^{-2}) but not TRF2 deletion (**d**). **e**, Metaphase spreads of MEFs of the indicated genotype and treatment were stained for telomeric DNA (green) and DAPI (red).

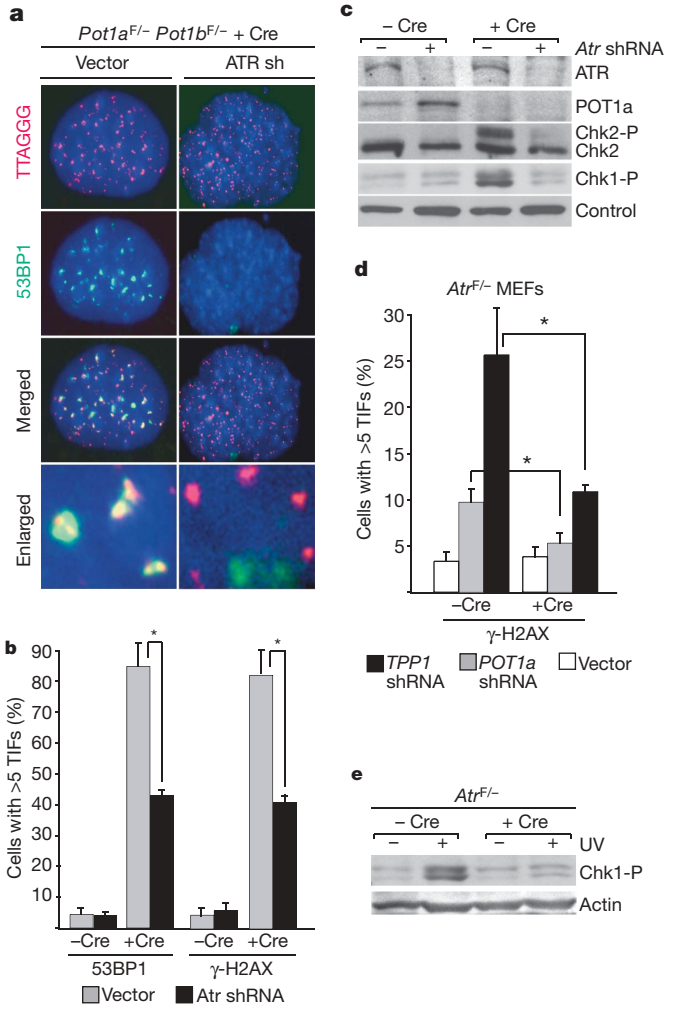

Figure 2 | POT1 inhibition activates ATR. **a**, 53BP1-positive TIFs in *POT1a/b* double knockout (DKO) MEFs with or without *ATR* shRNA. *Pot1a* and *b* were deleted with Adeno-Cre. **b**, Quantification of cells with five or more 53BP1-positive or γH2AX-positive TIFs (mean and s.d. of triplicate experiments; $n \geq 150$; asterisk, $P < 0.005$ based on a two-tailed Student's *t*-test). **c**, Immunoblotting for ATR, POT1a, Chk2 and Chk1-P in MEFs after the indicated treatment. **d**, TIFs in $Atr^{F/-}$ MEFs expressing *Pot1a* sh3 or *Tpp1* sh3. TIFs were detected by FISH–immnofluorescence either before (–Cre) or 4 d after (+Cre) infection with pWZL–Cre. Cells with five or more γH2AX TIFs were scored as positive (error bars, s.e.m.; $n \geq 150$, asterisk, $P < 0.01$ based on a two-tailed Student's *t*-test). **e**, Immunoblotting for Chk1-P in $Atr^{F/-}$ MEFs treated as indicated.

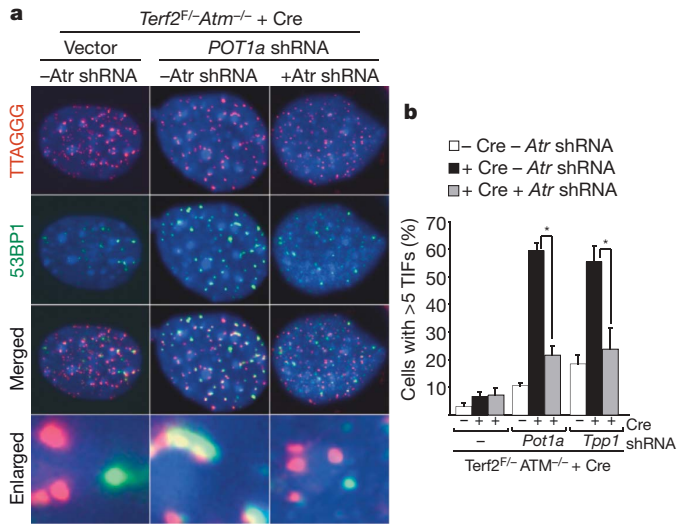

Figure 3 | ATR activation in *Terf2*$^{-/-}$*Atm*$^{-/-}$ cells on inhibition of POT1a. *Atm*$^{-/-}$*Terf2*$^{F/-}$ MEFs were infected with shRNAs to inhibit POT1a, TPP1 or ATR as indicated. TRF2 was deleted with a Cre adenovirus and TIFs were detected and quantified 5 d later as described in Fig. 1. **a**, **b**, Visualization and quantification of the effect of *Atr* shRNA on TIFs induced by inhibition of POT1a or TPP1 in *Atm*$^{-/-}$*Terf2*$^{F/-}$ cells. Error bars, s.d.; $n \geq 150$; asterisk, $P < 0.01$ based on a two-tailed Student's *t*-test.

Consistent with the data obtained in mouse cells, the telomere damage response resulting from inhibition of human POT1 was largely dependent on ATR (Supplementary Fig. 7). Collectively, these data show that ATR signalling at mammalian telomeres is repressed by POT1 proteins.

The data described above predict that the lack of ATR activation in *Terf2*$^{-/-}$*Atm*$^{-/-}$ MEFs is due to residual POT1a at the telomeres (Supplementary Fig. 2). To test this, we used shRNA to inhibit POT1a or TPP1 in *Terf2*$^{-/-}$*Atm*$^{-/-}$ cells. As deletion of POT1b does not induce a DNA damage response[18], we used a *Pot1b* shRNA as a negative control. We found that inhibition of POT1a or TPP1, but not POT1b, elicited a telomere damage response in *Terf2*$^{-/-}$*Atm*$^{-/-}$ cells (Supplementary Fig. 8a, b). We next tested the involvement of ATR in this response using an *Atr* shRNA in conjunction with either *Pot1a* or *Tpp1* shRNA. Two selectable markers were used to ensure the presence of both shRNAs. The results indicated that ATR signalling contributes to TIF formation when POT1a or TPP1 are compromised in *Terf2*$^{-/-}$*Atm*$^{-/-}$ cells (Fig. 3a, b). These data further confirm the role of POT1 in the repression of ATR and show that the TRF2-independent recruitment of POT1 or TPP1 is sufficient to repress ATR activation.

Unexpectedly, inhibition of POT1a or TPP1 in *Terf2*$^{-/-}$*Atm*$^{-/-}$ cells resulted in frequent telomere fusions (Fig. 4a, Supplementary Fig. 9). Telomere fusions occurred on 18 and 36% of chromosomes when cells were treated with *Pot1a* and *Tpp1* shRNAs, respectively. This is a significant increase from the background level of telomere fusions in *Terf2*$^{-/-}$*Atm*$^{-/-}$ cells (4% of chromosomes; Fig. 4a, Supplementary Fig. 9a). The occurrence of telomere fusions was not anticipated as *Pot1a/b* double knockout cells have a very weak telomere fusion phenotype[18]. Knockdown of POT1a or TPP1 did not induce telomere fusions in *Atm*$^{-/-}$ cells with normal TRF2 levels or in wild-type cells (Supplementary Fig. 9a), confirming previous findings that telomere fusions are effectively blocked by TRF2. The stimulation of telomere fusion by loss of POT1a from *Terf2*$^{-/-}$*Atm*$^{-/-}$ cells was also detected in genomic blots (Supplementary Fig. 9b). Inhibition of TPP1 led to a more severe telomere fusion phenotype than did *Pot1a* shRNA. This could be due to more effective removal of POT1a from telomeres through TPP1, the additional removal of POT1b, or other effects of TPP1 inhibition. Because NHEJ of telomeres after TRF2 deletion involved signalling by ATM, we investigated whether ATR signalling contributes to the NHEJ pathway that joins telomeres on POT1a loss from *Terf2*$^{-/-}$*Atm*$^{-/-}$ cells. Inhibition of ATR with shRNA partially suppressed the telomere fusions induced by inhibition of POT1a or TPP1 (Fig. 4a, Supplementary Fig. 9a).

Collectively, these data show that TRF2 and POT1 function independently to repress the activation of the ATM and ATR kinases at natural chromosome ends (Fig. 4b). How TRF2 prevents activation of the ATM kinase is not yet clear, although it has been suggested that TRF2, through its ability to interact with ATM, might block its activation[24]. We speculate that the ATR pathway is inhibited by POT1 by blocking the binding of RPA to the single-stranded telomeric DNA. Although RPA is more abundant, POT1 could be an effective competitor because of its shelterin-mediated enrichment at telomeres. The repression of ATM and ATR by TRF2 and POT1 explains how cells detect critically shortened telomeres. Because the abundance of shelterin at telomeres depends on the length of the duplex telomeric repeat array, short telomeres contain less TRF2 and POT1 (ref. 25). This diminished loading of TRF2 and POT1 is expected ultimately to lead to derepression of the ATM and ATR kinases, resulting in cell cycle arrest and inappropriate DNA repair at telomeres.

The dissection of the DNA damage response at mammalian telomeres also sheds light on the interplay between the ATM and ATR kinases. We show that ATM is not required for the activation of ATR, because removal of POT1 leads to an ATR response in *Atm*$^{-/-}$

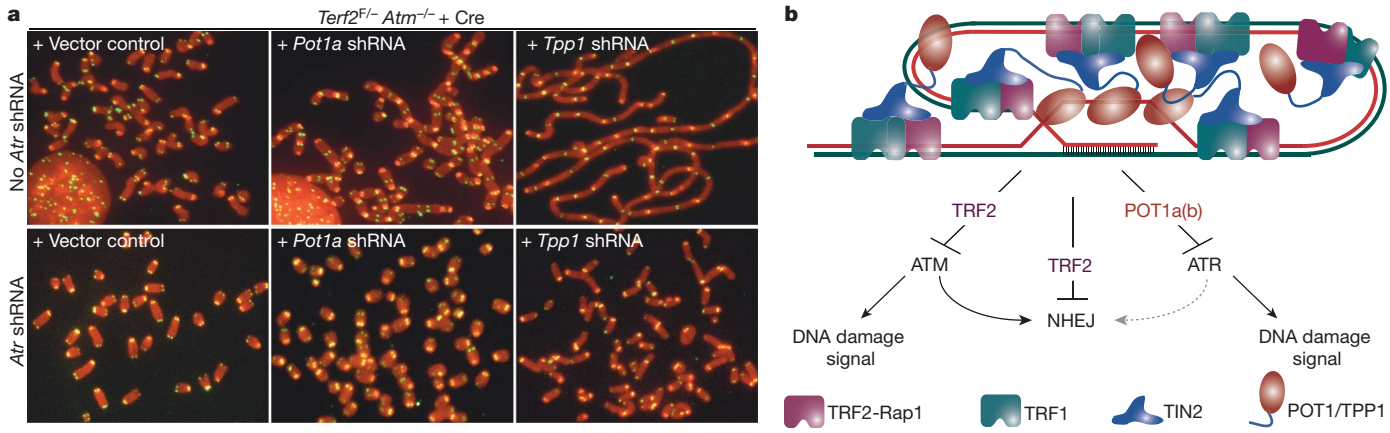

Figure 4 | Role of POT1 and ATR in NHEJ of telomeres lacking TRF2. *Terf2*$^{-/-}$*Atm*$^{-/-}$ cells were treated with shRNAs to modulate the levels of POT1a, TPP1 and ATR as described in Fig. 3. **a**, Telomere fusions visualized in metaphase spreads stained for telomeric DNA (green) and DAPI (red). **b**, Model for repression of the DNA damage response at telomeres. ATM and ATR are independently repressed by TRF2 and POT1. NHEJ is repressed by TRF2. NHEJ of telomeres lacking TRF2 is stimulated by either ATM or ATR signalling.

cells. This finding contrasts with the situation at irradiation-induced DSBs, where ATM signalling can promote activation of the ATR kinase, possibly by stimulating the formation of single-stranded DNA at the broken end[12]. At telomeres, which normally contain single-stranded DNA, such processing might not be necessary. Conversely, ATR is not required for the activation of ATM at telomeres. When TRF2 is removed from telomeres, ATM is activated without a contribution of ATR, which remains repressed by the residual POT1 at the chromosome ends.

Finally, our data reveal an unanticipated dependence of telomere fusions on signalling by either ATM or ATR (Fig. 4b). NHEJ of dysfunctional telomeres is primarily repressed by TRF2, possibly because the t-loop configuration blocks the end-loading of the Ku70/80 complex[26,27]. However, when TRF2 is deleted in $Atm^{-/-}$ cells, telomere NHEJ is inefficient. Whereas POT1 loss *per se* does not induce telomere fusions as long as TRF2 is functional, POT1 inhibition in $Terf2^{-/-}Atm^{-/-}$ cells does. Our data indicate that the key event in this setting is the activation of ATR. We therefore suggest that NHEJ at telomeres requires both the loss of TRF2 and the activation of either ATM or ATR (Fig. 4b). It is possible that the dependencies described here for NHEJ at dysfunctional telomeres might also hold for other forms of DNA damage. The modest effect of ATM deficiency on NHEJ in other settings[28] might be due to compensation by ATR signalling. Because the ATM and ATR kinase pathways are controlled separately by TRF2 and POT1, telomeres provide a unique opportunity to manipulate these pathways and to uncover regulatory interactions that otherwise might remain obscured.

METHODS

MEFs from E13.5 embryos obtained from crosses between $Atm^{+/-}$ (Jackson Labs) and $Terf2^{F/-8}$ mice were immortalized at passage 2 with pBabeSV40LT (a gift from G. Hannon). Cre was introduced by retroviral infection using Hit&Run *Cre–GFP* or *pWzl–Cre* expression vectors or using adenoviral infections with the Ad5 CMV Cre virus (Resource Centre, The University of Iowa). *Mx*–Cre mediated deletion of TRF2 from quiescent hepatocytes was performed as described[11]. Protein and genomic DNA were isolated 4 days after pI-pC induction of Cre.

ChIP[25,29], immunoblotting[8], immunofluorescence[8] and fluorescent *in situ* hybridization (FISH)/immunofluorescence co-staining[5] were performed as described using the following antibodies: TRF2 (1254); Rap1 (1252), TRF1 (644); POT1a (1220); TPP1 (1550); Chk2 (BD biosciences); Phospho-Chk1 (Ser 345) (Cell Signaling); ATR (N-19) (Santa Cruz); 53BP1 antibody (Novus, NB 100-304); γH2AX (Upstate Biotechnology); γtubulin (Sigma); and actin (Santa Cruz). Cells with at least five telomeric 53BP1 (or γH2AX) foci were scored as TIF positive; $n \geq 150$ for each experiment. Data reported are averages of three independent experiments.

shRNAs were expressed using a pSuperior-puromycin retroviral vector (OligoEngine) or (for ATR) the same vector modified to contain the hygromycin marker. Target sequences: *Atr* (sh3-1), GGAGATGCAACTCGTTTAA; *Tpp1* (sh3; ref. 21), GGACACATGGGCTGACGGA; *Pot1a* (sh3; ref. 18): GCATTTC-TCTACAACATTA.

Mouse telomeric DNA was analysed on CHEF gels[8] and by FISH[18] using previously described protocols.

Received 2 May; accepted 5 July 2007.
Published online 8 August 2007.

1. de Lange, T. Shelterin: the protein complex that shapes and safeguards human telomeres. *Genes Dev.* **19,** 2100–2110 (2005).
2. d'Adda di Fagagna, F. *et al.* A DNA damage checkpoint response in telomere-initiated senescence. *Nature* **426,** 194–198 (2003).
3. Karlseder, J., Broccoli, D., Dai, Y., Hardy, S. & de Lange, T. p53- and ATM-dependent apoptosis induced by telomeres lacking TRF2. *Science* **283,** 1321–1325 (1999).
4. Takai, H., Smogorzewska, A. & de Lange, T. DNA damage foci at dysfunctional telomeres. *Curr. Biol.* **13,** 1549–1556 (2003).
5. Herbig, U., Jobling, W. A., Chen, B. P., Chen, D. J. & Sedivy, J. M. Telomere shortening triggers senescence of human cells through a pathway involving ATM, p53, and p21(CIP1), but not p16(INK4a). *Mol. Cell* **14,** 501–513 (2004).
6. Qi, L. *et al.* Short telomeres and ataxia-telangiectasia mutated deficiency cooperatively increase telomere dysfunction and suppress tumorigenesis. *Cancer Res.* **63,** 8188–8196 (2003).
7. Wong, K. K. *et al.* Telomere dysfunction and Atm deficiency compromises organ homeostasis and accelerates ageing. *Nature* **421,** 643–648 (2003).
8. Celli, G. B. & de Lange, T. DNA processing not required for ATM-mediated telomere damage response after TRF2 deletion. *Nature Cell Biol.* **7,** 712–718 (2005).
9. Smogorzewska, A. & de Lange, T. Different telomere damage signaling pathways in human and mouse cells. *EMBO J.* **21,** 4338–4348 (2002).
10. Barlow, C. *et al. Atm*-deficient mice: a paradigm of ataxia telangiectasia. *Cell* **86,** 159–171 (1996).
11. Lazzerini Denchi, E., Celli, G. & de Lange, T. Hepatocytes with extensive telomere deprotection and fusion remain viable and regenerate liver mass through endoreduplication. *Genes Dev.* **20,** 2648–2653 (2006).
12. Jazayeri, A. *et al.* ATM- and cell cycle-dependent regulation of ATR in response to DNA double-strand breaks. *Nature Cell Biol.* **8,** 37–45 (2006).
13. Dimitrova, N. & de Lange, T. MDC1 accelerates nonhomologous end-joining of dysfunctional telomeres. *Genes Dev.* **20,** 3238–3243 (2006).
14. Zou, L. & Elledge, S. J. Sensing DNA damage through ATRIP recognition of RPA-ssDNA complexes. *Science* **300,** 1542–1548 (2003).
15. Bertuch, A. A. & Lundblad, V. The maintenance and masking of chromosome termini. *Curr. Opin. Cell Biol.* **18,** 247–253 (2006).
16. Enomoto, S., Glowczewski, L. & Berman, J. MEC3, MEC1, and DDC2 are essential components of a telomere checkpoint pathway required for cell cycle arrest during senescence in *Saccharomyces cerevisiae. Mol. Biol. Cell* **13,** 2626–2638 (2002).
17. Garvik, B., Carson, M. & Hartwell, L. Single-stranded DNA arising at telomeres in *cdc13* mutants may constitute a specific signal for the *RAD9* checkpoint. *Mol. Cell. Biol.* **15,** 6128–6138 (1995).
18. Hockemeyer, D., Daniels, J. P., Takai, H. & de Lange, T. Recent expansion of the telomeric complex in rodents: Two distinct POT1 proteins protect mouse telomeres. *Cell* **126,** 63–77 (2006).
19. Wu, L. *et al.* Pot1 deficiency initiates DNA damage checkpoint activation and aberrant homologous recombination at telomeres. *Cell* **126,** 49–62 (2006).
20. Brown, E. J. & Baltimore, D. Essential and dispensable roles of ATR in cell cycle arrest and genome maintenance. *Genes Dev.* **17,** 615–628 (2003).
21. Hockemeyer, D. *et al.* Telomere protection by mammalian POT1 requires interaction with TPP1. *Nature Struct. Mol. Biol.* advanced online publication, doi:10.1038/nsmb1270 (15 July 2007).
22. Cortez, D., Guntuku, S., Qin, J. & Elledge, S. J. ATR and ATRIP: partners in checkpoint signaling. *Science* **294,** 1713–1716 (2001).
23. Hockemeyer, D., Sfeir, A. J., Shay, J. W., Wright, W. E. & de Lange, T. POT1 protects telomeres from a transient DNA damage response and determines how human chromosomes end. *EMBO J.* **24,** 2667–2678 (2005).
24. Karlseder, J. *et al.* The telomeric protein TRF2 binds the ATM kinase and can inhibit the ATM-dependent DNA damage response. *PLoS Biol.* **2,** E240 (2004).
25. Loayza, D. & de Lange, T. POT1 as a terminal transducer of TRF1 telomere length control. *Nature* **423,** 1013–1018 (2003).
26. Celli, G. B., Lazzerini Denchi, E. & de Lange, T. Ku70 stimulates fusion of dysfunctional telomeres yet protects chromosome ends from homologous recombination. *Nature Cell Biol.* **8,** 885–890 (2006).
27. Griffith, J. D. *et al.* Mammalian telomeres end in a large duplex loop. *Cell* **97,** 503–514 (1999).
28. Lobrich, M. & Jeggo, P. A. Harmonising the response to DSBs: a new string in the ATM bow. *DNA Repair (Amst.)* **4,** 749–759 (2005).
29. Ye, J. Z. *et al.* POT1-interacting protein PIP1: a telomere length regulator that recruits POT1 to the TIN2/TRF1 complex. *Genes Dev.* **18,** 1649–1654 (2004).

Supplementary Information is linked to the online version of the paper at www.nature.com/nature.

Acknowledgements We thank D. White for invaluable help in maintaining our mouse colonies, D. Argibay for assistance with genotyping, E. Brown for providing the ATR conditional knockout mice, H. Takai for technical advice and suggestions, D. Hockemeyer for providing *Pot1* double knockout cells and the *Tpp1* and *Pot1a* shRNA constructs, S. Soll for his contributions to the initial stages of this research and members of the de Lange laboratory for critical comments on the manuscript. This work was supported by a grant from the NIH.

Author Information Reprints and permissions information is available at www.nature.com/reprints. The authors declare no competing financial interests. Correspondence and requests for materials should be addressed to T.deL. (delange@mail.rockefeller.edu).

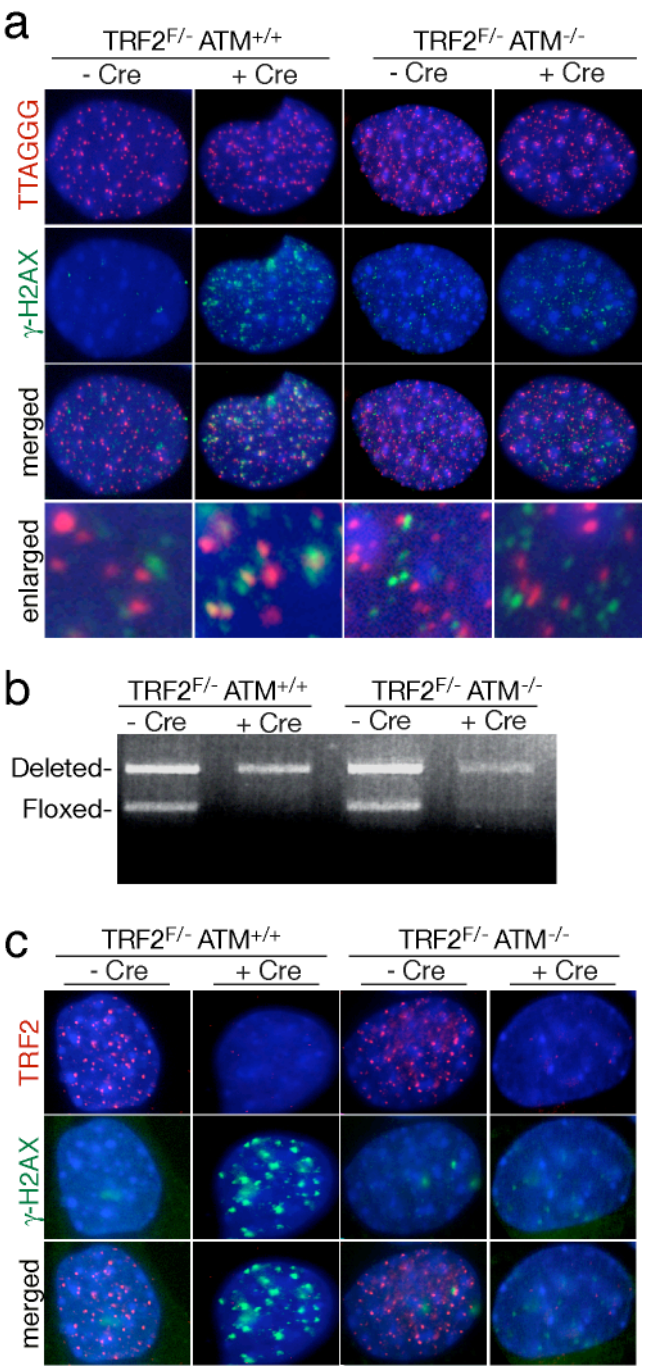

Supplementary Figure 1. ATM-dependent DNA damage signal at telomeres lacking TRF2. a, MEFs of the indicated genotype were untreated (-Cre) or infected with a self-deleting Cre expression vector (Hit&Run Cre) (+ Cre) and harvested 5 days post infection. Cells were stained for telomeric DNA (red), γ-H2AX (green) and DAPI (blue). **b**, PCR on genomic DNA isolated form cells of the indicated genotype and treatment analyzed for Cre mediated recombination of the TRF2 locus. **c,** MEFs of the indicated genotype were treated as described in panel a and stained for TRF2 (red), γ-H2AX (green) and DAPI (blue).

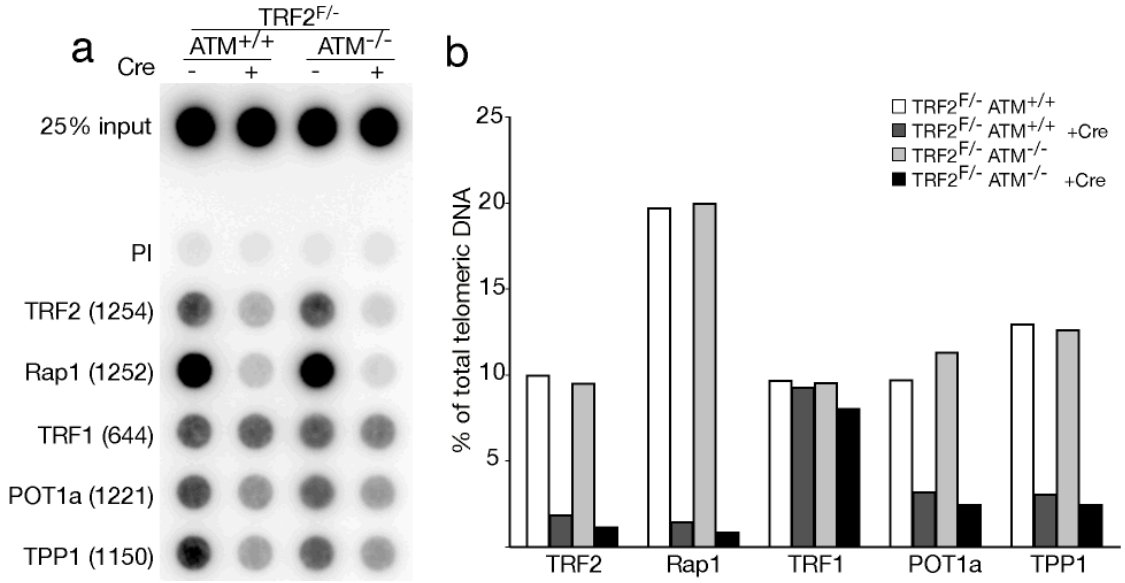

Supplementary Figure 2. Shelterin status in ATM proficient and ATM deficient cells following TRF2 deletion. a, Chromatin immunoprecipitation using antibodies raised against the indicated proteins before or after TRF2 deletion in $ATM^{-/-}$ or $ATM^{+/+}$ MEFs. Cells were harvested either prior of 5 days following pWZL-Cre infection. **b,** Quantification of the data presented in (**a**) expressed as % of total telomeric DNA. The specificity of the antibodies used in this experiment was previously shown (Hockemeyer et al. Cell, 2006).

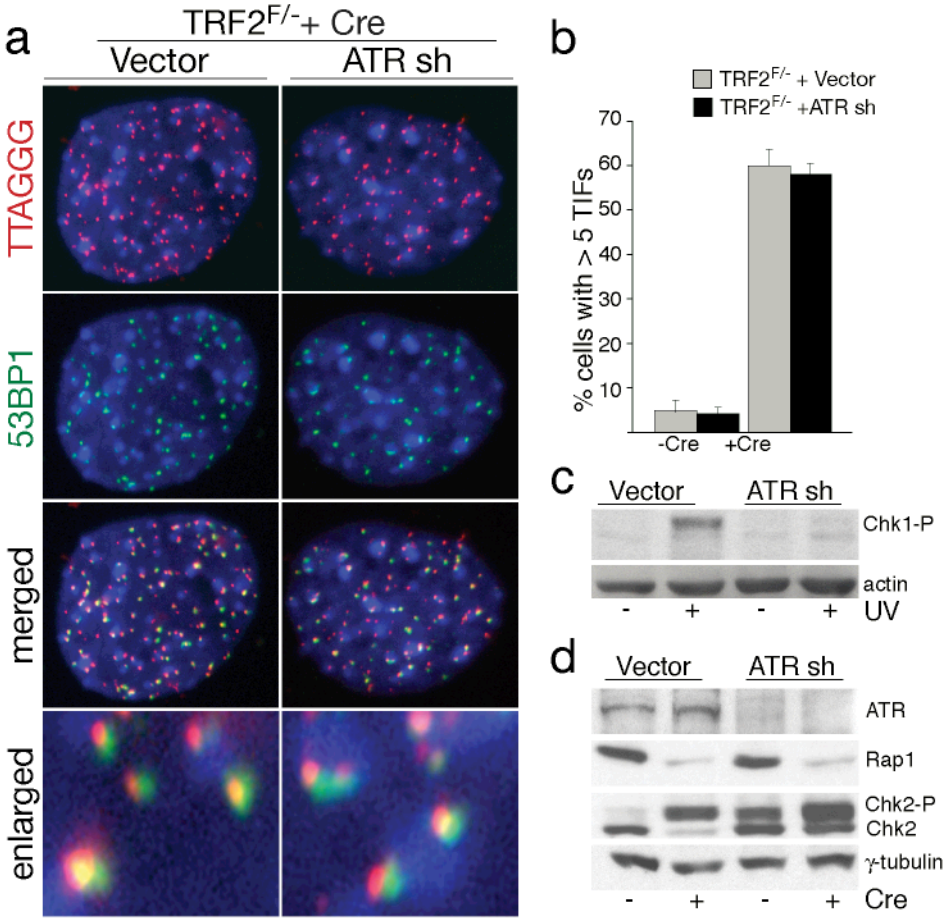

Supplementary Figure 3. ATR-independent DNA damage signal at telomeres lacking TRF2. a, Effect of ATR shRNA on TIFs in TRF2$^{F/-}$ MEFs infected with Ad-Cre adenovirus. **b,** Quantification of data in (**a**) (average and SD of triplicate experiments, n≥150). **c-d,** Immunoblots showing abrogation of UV-induced Chk1 phosphorylation in MEFs expressing ATR shRNA (**c**), ATR, Rap1 and Chk2 levels (**d**) upon TRF2 deletion from cells infected with and without ATR shRNA.

a

Genotype	Cre	Chromosomes analyzed			Telomere Fusions			Fusions/ chromosome
Experiment		I	II	III	I	II	III	
$TRF2^{F/-}$ $ATM^{+/+}$	-	373	734	821	0	1	0	0.00
	+	654	810	1590	350	570	911	0.60± 0.09
$TRF2^{F/-}$ $ATM^{-/-}$	-	510	978	1010	0	1	1	0.00
	+	790	1218	1579	23	56	68	0.04± 0.01

b

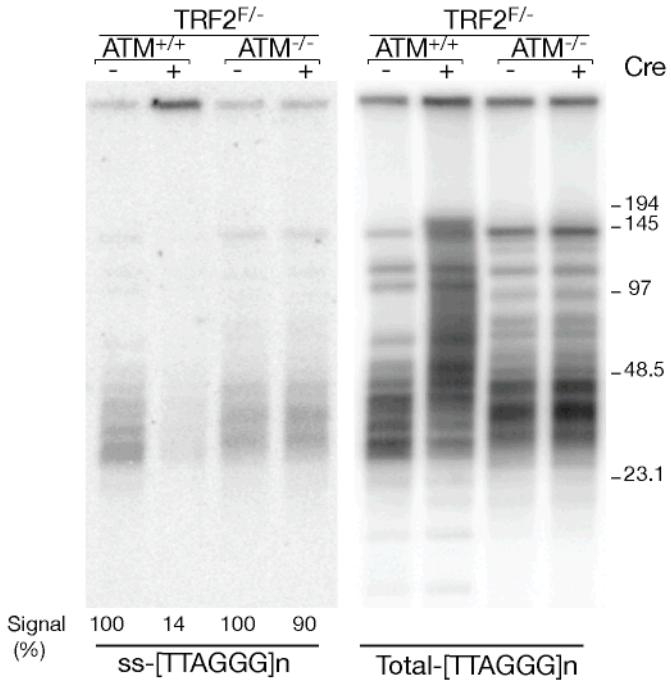

Supplemental 4. Inefficient NHEJ-mediated telomere fusions in ATM null cells. a, Telomere fusions were quantified by FISH analysis of metaphase spreads obtained from MEFs of the indicated genotype, representative images of the data analyzed are shown in Fig. 1e. Cells were harvested before or 96 hours post Cre infection. **b,** In-gel detection of telomeric restriction fragments from MEFs of the indicated genotype and treatment. Left: detection of the 3' overhang under native conditions. Right: total telomeric hybridization signal obtained after in situ DNA denaturation. Probe: $[CCCTAA]_4$. Normalized 3' overhang signals are shown bottom left

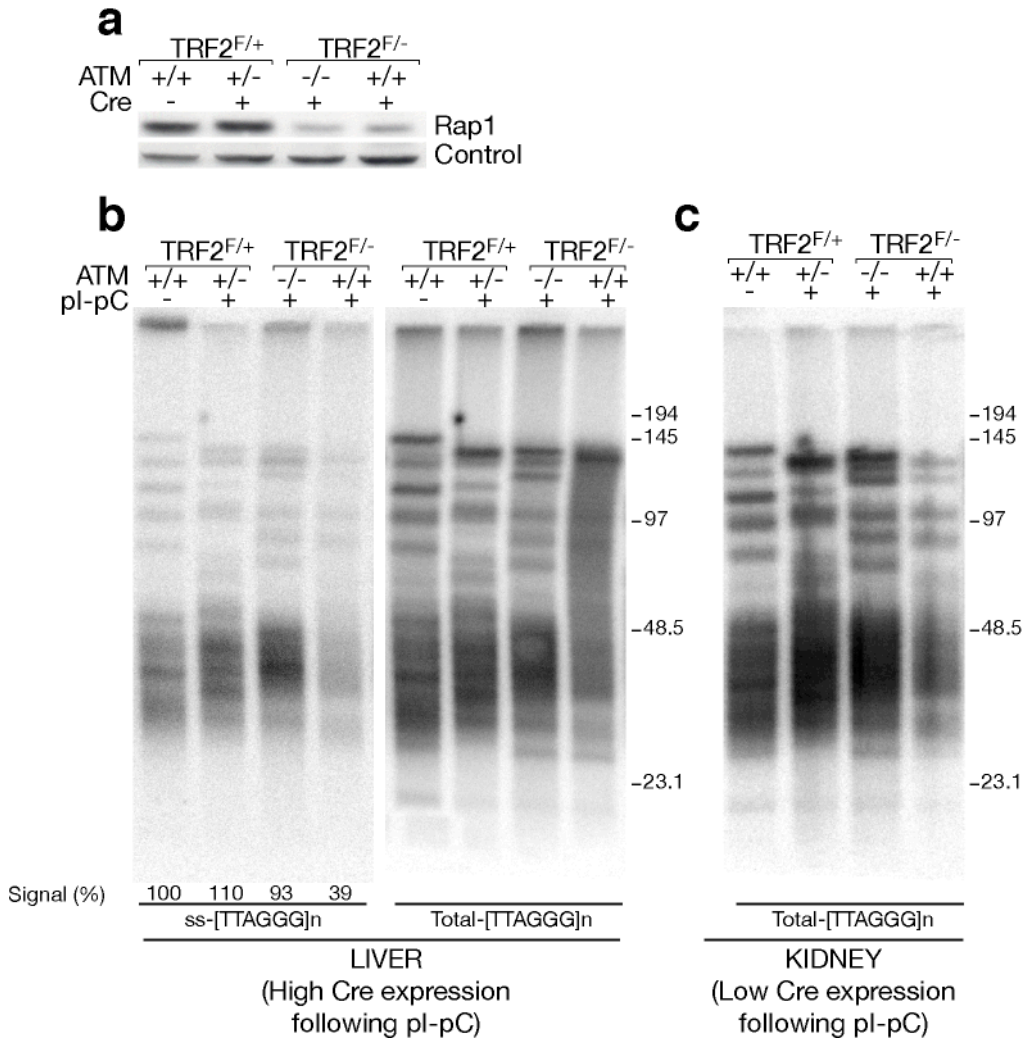

Supplementary Figure 5. ATM promotes telomere fusions *in vivo.* a, Immunoblotting for Rap1 loss following Cre-mediated TRF2 deletion in the liver of $ATM^{-/-}$ or $ATM^{+/+}$ Mx-Cre transgenic mice. Livers were isolated 9 days post pI-pC-mediated induction of Cre. **b,** Genomic DNA isolated from livers of the indicated genotypes treated as in panel (a) was analyzed by in-gel telomere blotting. The left image shows hybridization signal using the TelC probe ($[CCCTAA]_4$) under native conditions detecting the telomeric 3' overhang. The right image shows the total telomeric hybridization signal obtained with the same probe after in-gel denaturation of the DNA. **c,** As an internal control genomic DNA of the same mice was isolated kidney which shows no Cre-mediated recombination. Total telomeric hybridization signal is shown.

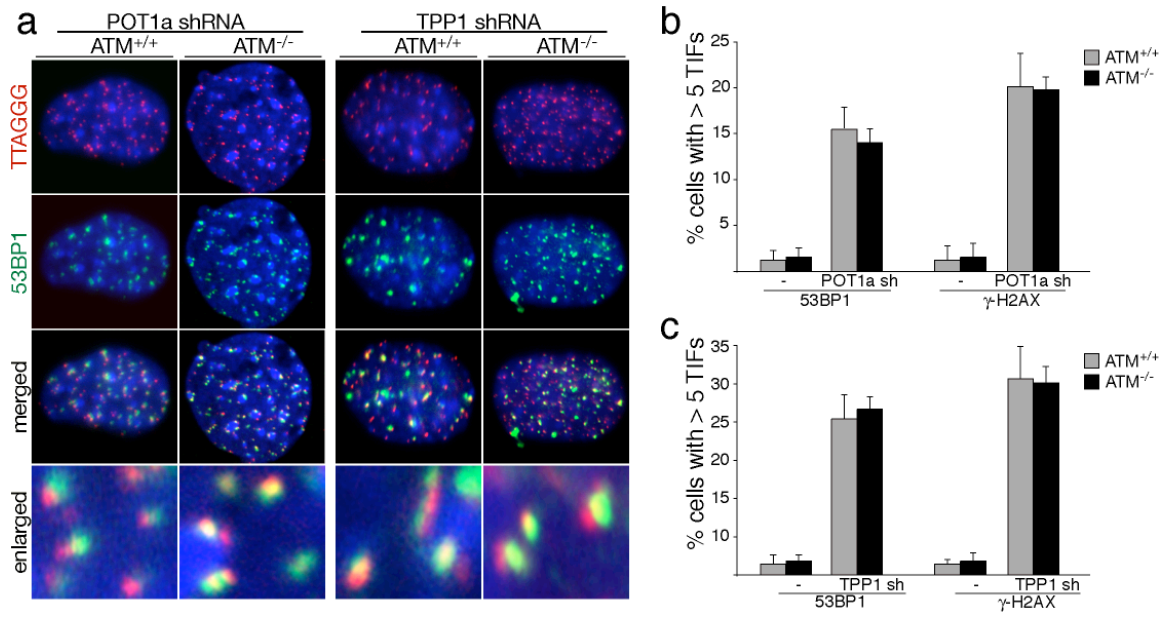

Supplemental 6 ATM-independent DNA damage response at telomeres lacking POT1. a, 53BP1 TIFs in cells of the indicated genotype infected with either POT1 or TPP1 shRNA. **b-c,** Quantification of the effect of ATM status on 53BP1 and γ–H2AX TIFs induced by inhibition of POT1a and TPP1 (average and SD of triplicate experiments, n≥150).

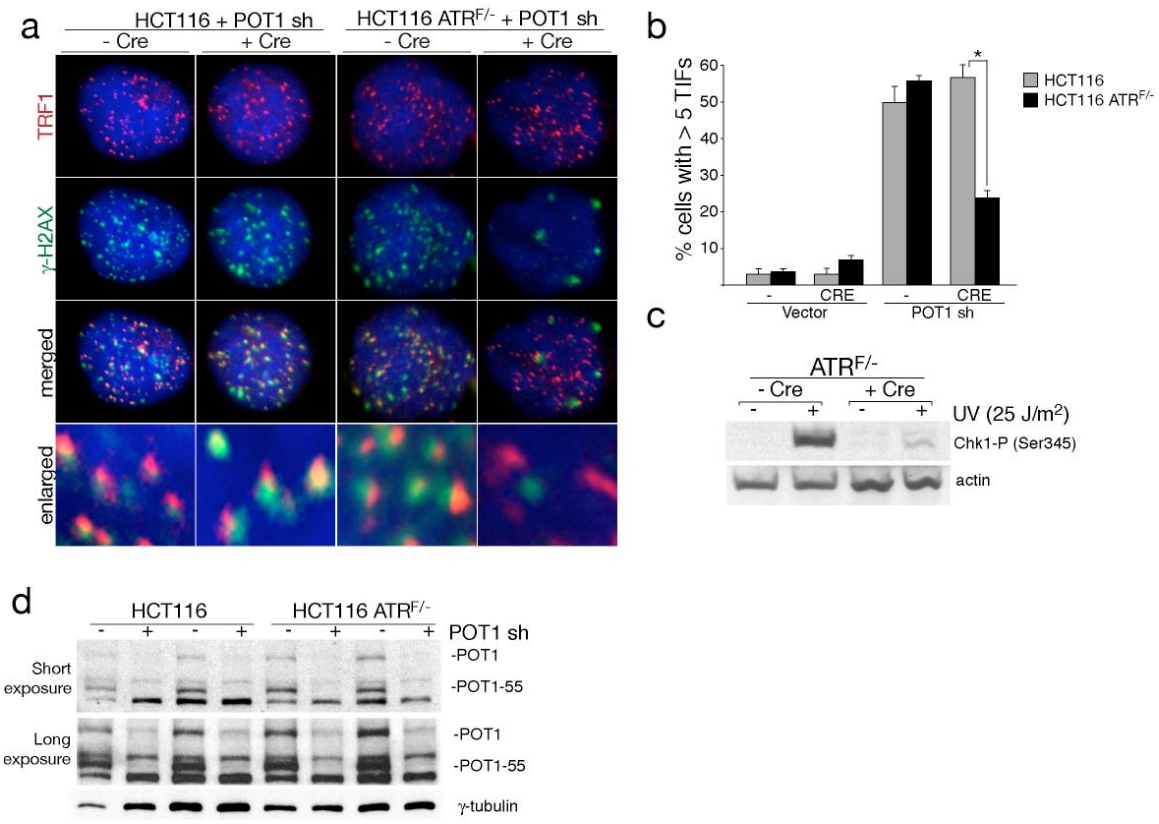

Supplementary Figure 7. Activation of ATR in human HCT116 cells treated with POT1 shRNA. a, HCT116 ATR$^{Fl/-}$ cells and parental HCT116 were infected with POT1 shRNA and either uninfected (-Cre) or infected with a Cre Adenovirus (+Cre). Four days later cells were stained for TRF1 DNA (red), γ-H2AX (green) and DAPI (blue). **b,** Quantification of cells with > than 5 γ-H2AX foci at telomeres. (Error bars= SD; n≥150; asterisk, $P < 0.005$ based on a two-tailed Student's *t*-test). **c,** Immunoblotting for Chk1-P in HCT116 ATR$^{Fl/-}$ cells either untreated or Cre infected before or after UV treatment. **d,** Immunoblot for the expression of POT1 and POT1-55 in the cells with indicated genotype before or after POT1 shRNA.

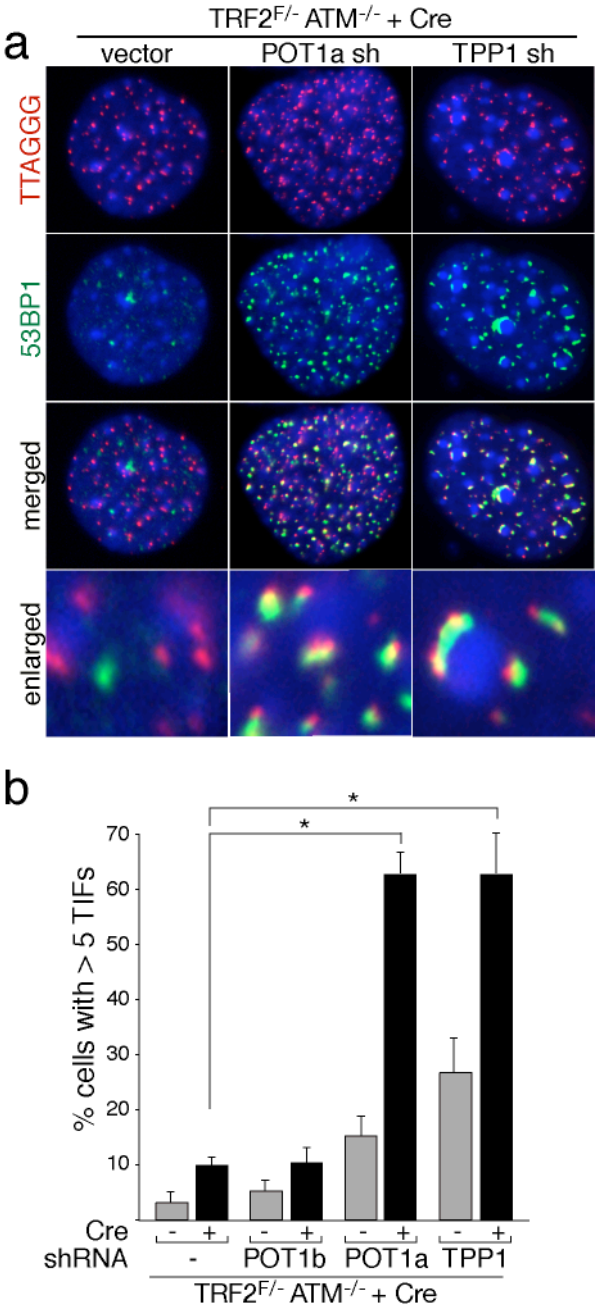

Supplementary Figure 8. Induction of DNA damage in TRF2$^{-/-}$ ATM$^{-/-}$ upon POT1 inhibition. a, ATM$^{-/-}$TRF2$^{F/-}$ MEFs were infected with shRNAs for either POT1a or TPP1 as indicated. TRF2 was deleted with a Cre adenovirus and TIFs were detected and quantified 5 days later. **b**, Quantification of TIFs induced by POT1a or TPP1 inhibition in TRF2$^{-/-}$ATM$^{-/-}$ cells. (average and SD of triplicate experiments; n≥150; asterisk, $P < 0.001$ calculated using a two-tailed Student's *t*-test).

a

Genotype	Cre	ATR shRNA	Chromosomes analyzed	Telomere fusions		Fusions/ chromosome
$TRF2^{F/-}$ $ATM^{+/+}$	-	-	1107	2		0.00
	+	-	1745	1037		0.59
$TRF2^{F/-}$ $ATM^{-/-}$	-	-	1010	1		0.00
	+	-	1574	62	p=0.139	0.04
	+	+	1314	38		0.03
$TRF2^{F/-}$ $ATM^{-/-}$ +POT1a sh	-	-	849	0		0.00
	+	-	1992	358	p<0.001	0.18
	+	+	1465	151		0.10
$TRF2^{F/-}$ $ATM^{-/-}$ +TPP1 sh	-	-	753	1		0.00
	+	-	1804	650	p<0.001	0.36
	+	+	1532	274		0.18

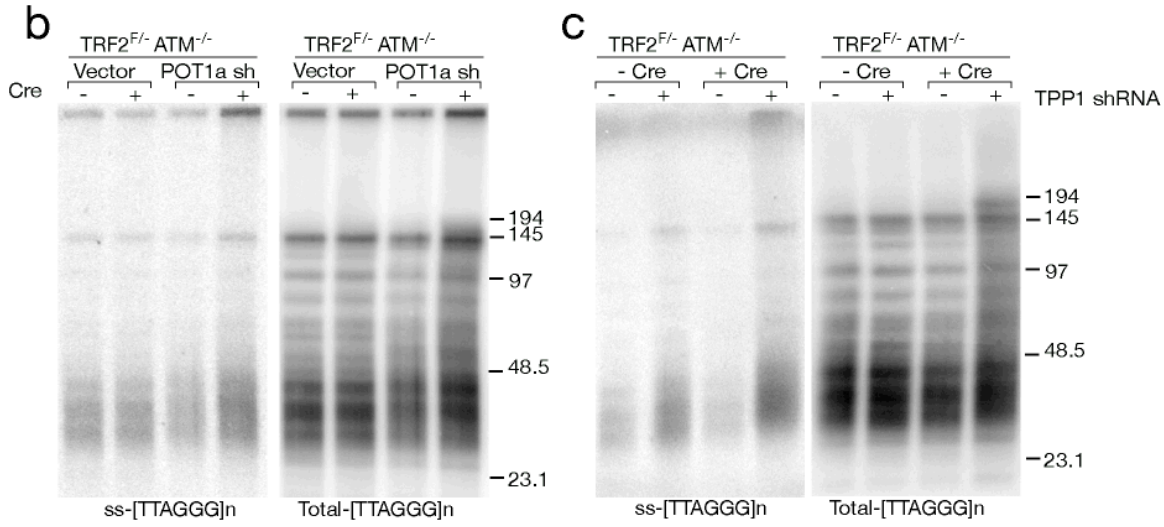

Supplementary Figure 9. Role of POT1 and ATR in NHEJ of telomeres lacking TRF2. a, $TRF2^{-/-}ATM^{-/-}$ cells were treated with shRNAs to modulate the levels of POT1a, TPP1, and ATR as described in Fig. 3. **a,** Telomere fusions were quantified by FISH analysis of metaphase spreads obtained from MEFs of the indicated genotype, representative images of the data analyzed are shown in Fig. 4**a. b-c**, In-gel detection of telomeric restriction fragments from $TRF2^{F/-}$ $ATM^{-/-}$ MEFs infected with either POT1a (**b**) or TPP1 (**c**) shRNA before or after Cre treatment. For each panel it is shown the detection of the 3' overhang under native conditions and the total telomeric hybridization signal obtained after in situ DNA denaturation. Probe: $[CCCTAA]_4$.